ECRONICON OPEN ACCESS

EC EMERGENCY MEDICINE AND CRITICAL CARE
Research Article

Detection of Brain Tumor Based on Extraction Feature Vectors

Samir Kumar Bandyopadhyay*

University of Calcutta, India

***Corresponding Author**: Samir Kumar Bandyopadhyay, University of Calcutta, India.

Received: November 28, 2019; **Published:** February 29, 2020

Abstract

It is a critical task for diagnosis and curing the brain tumour. The diagnosis of brain tumor requires a fast and efficient way to classify it through multiple stages. It is the aim of the paper to proposed a system for diagnosis the disease. MRI of brain as input is normalized. Next extraction of feature vectors from the image is made to reduce the redundancy of data for the classifier. Finally, each tuple of feature extracted vector is used for producing classified output. The proposed methodology is performed very efficiently and accurately.

Keywords: *Tumor; Metastatic Adenocarcinoma; Metastatic Bronchogenic and Carcinoma*

Introduction

Brain tumours are found the second most cause of cancer-related deaths in children and adults. A tumour is graded into several stages for the analysis of abnormality. It depends on the acute probability of tumour growth in size and its coverage. The grade can be analysis based on biopsy. Grading of the tumour is not same as cancer stages. Five major types of brain tumours are considered for computerized classification. A database has been created that contains images for testing and training the classifiers.

Literature Review

Researchers work on to classify brain tumours into appropriate types. Some researchers texture based analysis using Gabor wavelets is used to improve the accuracy of classification. Some others used Support Vector Machine (SVM) based classifier to classify the tumors [1]. Some authors also used discrete wavelet transforms on the MRI slices to extract the features and then Principal Component Analysis (PCA) was used to classify brain tumor [2]. Feed forward back propagation neural network and K-nearest neighbours are implemented for classification [1]. Other researchers use SVM with recursive feature elimination (SVM-RFE) for classification [3]. Ranking based criterion that tests the discriminative power of each distinct feature was used as SVM-RFE to produces an optimal performance for the classifier.

An implementation of image moseying in MRI brain abnormalities segmentation study are formed by cutting various shapes and size of abnormalities and pasting it onto normal brain tissue [2]. Some methods like ANFIS, FCM are used for segmentation of brain MRI. Receiver Operating Characteristic (ROC) used to calculate the accuracy. An automatic method [3] that integrates knowledge-based techniques with multispectral analysis for tumour labels identification. The back propagation learning algorithm is a supervised learning method that can be used with multilayer networks and nonlinear differentiable transfer functions. Neural network and ANN perform much better when dealing with multi-dimensions and continuous features [7-11]. In this paper, Adaptive based Neural network is used to classify the major five types of brain tumour from standard datasets with accuracy.

Proposed Methodology

Tumour detected MRI of brain slices is selected for classification. Artifacts and skull elimination is used to remove unnecessary regions of MRI. The model is first trained using training normalized dataset in classification step and it defines the class labels being used. After performing the training on a set of existing known data set then test the data for appropriate classes for detecting class of tumour. The implementation of the technique is shown in the figure 1.

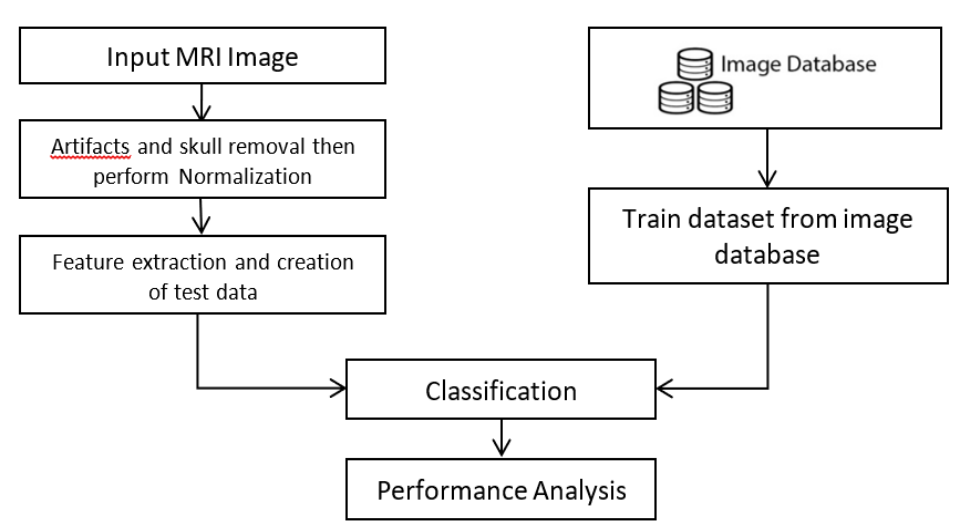

Figure 1: *Workflow of the tumour classification.*

The images have been collected from brain atlas [4] and other mentioned dataset [5-7]. Using random dataset the experiments is conducted.

Features Selection

Histogram of an image represents the concise statistical information contained in the image. f(x,y) represents the intensity level for each pixel (x,y) in the image $x = 1,2,\cdots, A \;\; y = 1,2,\cdots, B$. The equation (1) calculates probability density function for each occurring pixel intensity level $0,1,\cdots, N-1$:

$$p(i) = \frac{h(i)}{AB} \; for \; i = 0,1,\cdots, N-1 \quad (1)$$

$$h(i) = \sum_{x=1}^{A}\sum_{y=1}^{B}\delta(f(x,y),i) \quad (2)$$

Here $h(i)$ is the intensity level histogram function for the whole image and each intensity level i. Here we have taken $\delta(i, j)$ as the Kronecker delta function that can be given as:

$$\delta(i,j) = \begin{cases} 1, & i = j \\ 0, & i \neq j \end{cases} \quad (3)$$

The following parameters are used for extraction of features from image:

Mean: The average value of the intensity of the image and can be given as:

$$\mu = \sum_{i=0}^{N-1} i \cdot p(i) \qquad (4)$$

Variance: It measures intensity variation around mean and is represented by:

$$\sigma^2 = \sum_{i=0}^{N-1} (i-\mu)^2 p(i) \qquad (5)$$

Skewness: Gives us the measure of the amount of symmetry of the histogram around mean. It can be given by:

$$\mu_3 = \sigma^{-3} \sum_{i=0}^{N-1} (i-\mu)^3 p(i) \quad (6)$$

Kurtosis: Measures the flatness in the histogram and is given by:

$$\mu_4 = \sigma^{-4} \sum_{i=0}^{N-1} (i-\mu)^4 p(i) - 3 \qquad (7)$$

Entropy: Represents the uniformity of the histogram and is given by:

$$H = \sum_{i=0}^{N-1} p(i) \log_2 [p(i)] \qquad (8)$$

Energy: *R*epresents the mean of squared value of the pixel intensity and can be given as:

$$E = \sum_{i=0}^{N-1} [p(i)]^2 \quad (9)$$

Parameters as mentioned above are used for texture segmentation. Grey-level co-occurrence matrix $h_{d\theta}(i,j)$ i.e. second-order histogram is defined by probability distribution of pixel. The image matrix is divided by the total number of neighbouring pixels $R(d,\theta)$ in the image; the resulting image becomes the joint probability $p_{d\theta}(i,j)$ for two pixels with the distance d between them and along the direction i and value for $d = 1,2$ and $\theta = 0^\circ, 45^\circ, 90^\circ, 135^\circ$ is normally used. For a given image with intensity function $f(x,y)$ and N discrete intensity values, matrix $h_{d\theta}(i,j)$ and defining the parameters i and j as:

$f(x_1,y_1)=i$ and $f(x_2,y_2)$

where $(x_2, y_2) = (x_1, y_1) + (d\cos\theta, d\sin\theta)$ (11)

This results in a matrix dimension equal to the number of intensity levels as parameters and for each distance the orientation is θ. Parameters are derived from the matrix where μ_x, μ_y and σ_x, σ_y as the mean and standard deviation. The parameters are given as:

Angular second moment (energy): Energy also means uniformity or angular second moment. The more homogeneous the image is, the larger the value.

$$\sum_{i=0}^{N-1} \sum_{j=0}^{N-1} [p(i,j)]^2 \quad (12)$$

Correlation: It finds the correlation between two neighbour pixels. It is measured by:

$$\sum_{i=0}^{N-1}\sum_{j=0}^{N-1}\frac{ijp(i,j)-\mu_x\mu_y}{\sigma_x\sigma_y} \quad (13)$$

Inertia (Contrast): Contrast measures the intensity of local changes in an image. It reflects the sensitivity of the textures about the changes in the intensity. It is determined by:

$$\sum_{i=0}^{N-1}\sum_{j=0}^{N-1}(i-j)^2\,p(i,j) \quad (14)$$

Absolute value: Measures the intensities of the image.

$$\sum_{i=0}^{N-1}\sum_{j=0}^{N-1}|i-j|p(i,j) \quad (15)$$

Inverse Difference: Influenced by the homogeneity of the image. The result is a low inverse difference value for inhomogeneous images, and a relatively higher value for homogeneous images.

$$\sum_{i=0}^{N-1}\sum_{j=0}^{N-1}\frac{p(i,j)}{1+(i-j)^2} \quad (16)$$

Entropy: It measure variation of randomness of intensity in a image.

$$H=-\sum_{i=0}^{N-1}\sum_{j=0}^{N-1}p(i,j)\log_2[p(i,j)] \quad (17)$$

Using above discussed parameters feature vector generates that can help in classification of the input image into the predetermined class label.

Classification

Classification consists of learning phase and testing phase. In Learning phase, it needs to build a model that can successfully classify a dataset. Back propagation algorithm is an optimization procedure based on gradient descent. It adjusts the weights to reduce the system error. During the learning phase, input patterns are presented to the network, and the network parameters are changed to bring the actual outputs closer to the desired target values. Outputs are compared to the target values. Any difference indicates an error. This error is some scalar function of the weights. Thus, the weights are adjusted to reduce the error. This error function is the sum of square differences between the outputs and targets. Thus, the errors computed at the output layer are used to adjust the weights between the last hidden layer and the output layer.

The classification uses fuzzy rules and fuzzy reasoning. In the case of fuzzy if-then rules which take the following form:

$$if\ x\ is\ A\ then\ y\ is\ B \quad (18)$$

On the universe of discourse of x and y, A and B are denoted by linguistic values in fuzzy sets respectively. The statement "x is A" is called the premise and the statement "y is B" is called conclusion. The relation between two variables X and y in which the fuzzy rule defined as a binary relation R on the product space $X \times Y$. A typical Sugeno fuzzy [8] model is the following form of fuzzy rules:

$$if\ x\ is\ A\ and\ y\ is\ B\ then\ z = f(x, y)\ (19)$$

Here A and B are fuzzy rules and z=f(x,y) is a crisp on the input variables X and y . A two input fuzzy model is shown in figure 2.

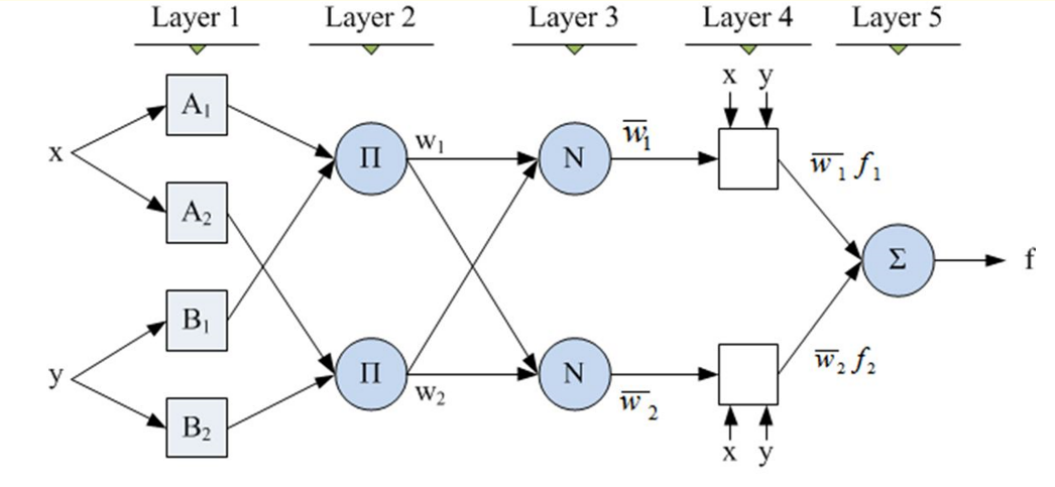

Figure 2: *Architecture of fuzzy inference system.*

The output $O_{l,i}$ is derived from each i[th] node in the particular layer *l* takes an input from the previous layer. This mapping function of each layer is as follows:

For layer 1 we take $l = 1$ and output as for each i[th] node in this layer. The node function is described as:

$$O_{1,i} = \begin{cases} \mu_{A_i}(x) & \text{for i} = 1,2 \\ \mu_{B_{i-2}}(y) & \text{for i} = 3,4 \end{cases} \quad (20)$$

Here X or y is the input variable to node *i* and each node is assigned a linguistic label A_i or B_{i-2} to it. Here $\mu_A(x)$ indicates the membership function for *A*.

In the next layer (Layer 2) we consider a fixed node label denoted by Π for which the output for the incoming signal can be defined by:

$$O_{2,i} = w_i = \mu_{A_i}(x)\mu_{B_i}(y) \qquad \text{for i} = 1,2 \ (21)$$

NN denotes a fixed node label for every node in layer 3. The normalized firing strengths for every i[th] node is calculated by the ratio of the firing strength of the corresponding layer to the sum of all firing rules present in that layer. It is given as:

$$O_{3,i} = \overline{w_i} = \frac{w_i}{\sum_{i=1}^{2} w_i} \ (22)$$

The output considering the parameter set embedded in the membership function is computed in layer 4. The parameters in this set are referred as consequent parameters. The node function of every i^{th} node can be given as:

$$O_{4,i} = \overline{w_i} f_i(x, y) \quad (23)$$

In the last layer (layer 5) each of the nodes is assigned with a fixed node label Σ . Each node computes the summation of all incoming signals as outputs as:

$$O_{5,i} = \sum_i \overline{w_i} f_i(x, y) = \frac{\sum_i w_i f_i(x, y)}{\sum_i w_i} \quad (24)$$

Results and Discussion

The methodology is implemented and tested on benchmark dataset [5-7]. The efficiency of the classifier is calculated based on the comparison made with predicted class to the actual class label. This methodology is tested on a personal computer.

The images are normalized to the feature vector and 12 features are extracted from the slices. Each of the feature vector forms an input tuple to the classifier. The classifier takes 20 input slices and forms input tuple based on each feature vector. The results are shown in figure 3. It is also illustrated by table 1 and 2.

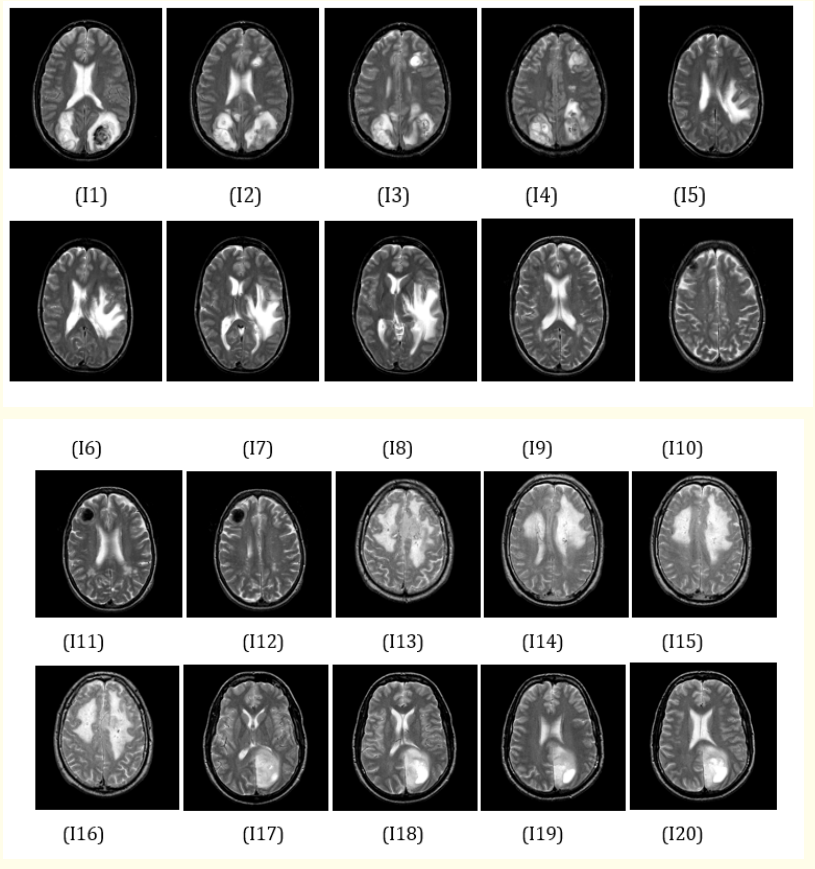

Figure 3: *20 input slices passed through the normalization and feature extraction processes for classification. After classification we found that slices I1-I4 are Type 1(Class 1) (Sarcoma); slicesI5-I8 are Type 2 (Class 2) (Meningioma); slices I9-I12 are ype 3 (class 3) (Metastatic adenocarcinoma); slices I13-I16 are Type 4 (Class 4) (Metastatic bronchogenic arcinoma);slicesI17-I20 are Type 5 (Class 5) (Glioma).*

1st order histogram based features and features from Gray Level Co-occurrence Matrix are used to generate each feature vector from the normalized grayscale image. These are the variation of intensity values based amongst the pixels in the selected slices. Different features of slices are shown in table 1 and 2.

Class label of each tuple denotes its tumour type which is used to build IF-THEN rules to generate the Artificial Neural Fuzzy Inference System. Based on the training tuples and the result from the inference system, an adaptive network is then built up. The model is trained using the network to generate the class label (as mentioned above in figure 3) for the input slices. The classifier gives fuzzy numbers as output. It is then de- fuzzified to get the actual class labelled values.

Performance measurement

By comparing the actual class labels and the predicted class labels based on True Positive (TP), True Negative (TN), False Positive (FP), False Negative (FN) and F-score for each of the individual classifiers are measured for performance calculation. Different performance parameters based on TP, TN, FP and FN are calculated to find such as Sensitivity, Accuracy, etc. Table 3 shows the performance measurement 5 major class of tumour types.

The performance of the classifiers is evaluated in terms of sensitivity, specificity, precision, accuracy and F-score. The average value of sensitivity is 0.90815166, the average value of specificity is 0.977151379, the average value of precision is 0.907038177, the average value of accuracy is 0.963461538, and the average value of F-score is 0.906558695 for the model.

Image sequence	Mean	Variance	Skewness	Kurtosis	Energy	Entropy
1	15.5399	446.433	0.000108	0.000127	0.2816	3.6817
2	14.7607	427.681	0.000126	0.000151	0.2933	3.5751
3	15.5426	447.411	0.000108	0.000127	0.2810	3.6939
4	15.3294	434.847	0.000116	0.00014	0.2762	3.7014
5	15.9980	466.920	0.0001	0.000118	0.2718	3.8210
6	16.2995	455.317	0.000972	0.000117	0.2540	3.8918
7	16.8535	461.050	0.000906	0.00011	0.2365	3.9722
8	15.2010	463.274	0.000113	0.000132	0.2981	3.6796
9	13.6257	406.182	0.00015	0.000185	0.3333	3.2856
10	13.9531	413.331	0.000143	0.000175	0.3219	3.4029
11	13.1538	400.748	0.000161	0.000200	0.3529	3.2298
12	14.2234	417.177	0.000137	0.000165	0.3123	3.4526
13	13.6782	420.489	0.000142	0.000167	0.3506	3.2687
14	13.5103	417.582	0.000144	0.000169	0.3583	3.1849
15	13.2064	412.893	0.000151	0.000178	0.3698	3.1134
16	12.3658	388.257	0.000181	0.000226	0.3857	3.0153
17	12.9241	397.207	0.000167	0.00021	0.3573	3.2094
18	13.5875	407.496	0.000151	0.000185	0.3342	3.3352
19	14.2193	425.415	0.000137	0.000164	0.3174	3.4692
20	14.9834	443.361	0.000118	0.000138	0.3040	3.5664

***Table 1**: Various Features from the normalized grayscale MR image.*

Image sequence	Contrast	Correlation	Energy	Homogeneity	Inverse difference	Absolute value
1	0.3334	0.3878	0.4131	0.8726	56710.6	17910
2	0.3190	0.3833	0.4379	0.8774	57036.6	17210
3	0.3415	0.3862	0.4071	0.8697	56512.8	18328
4	0.3547	0.3508	0.4112	0.8659	56247.2	18914
5	0.3618	0.3884	0.3971	0.8663	56246	18994
6	0.3499	0.3785	0.3871	0.8652	56218.6	18910
7	0.3697	0.3640	0.3731	0.8592	55806.6	19812
8	0.3610	0.3920	0.4227	0.8712	56534.6	18504
9	0.2931	0.3803	0.4756	0.8861	57632.2	15936
10	0.2984	0.3755	0.4668	0.8831	57439.6	16314
11	0.2885	0.3749	0.4930	0.8896	57854	15516
12	0.3019	0.3595	0.4589	0.8800	57245.4	16676
13	0.2558	0.4260	0.4907	0.8970	58395.4	14258
14	0.2565	0.4179	0.4908	0.8972	58406	14248
15	0.2443	0.4349	0.5019	0.9011	58674.6	13668
16	0.2395	0.4074	0.5274	0.9029	58796.6	13412
17	0.2881	0.3883	0.4918	0.8902	57893.2	15446
18	0.2936	0.3933	0.4727	0.8867	57670.4	15878
19	0.3158	0.3685	0.4617	0.8804	57227	16858
20	0.3164	0.3804	0.4429	0.8786	57115.6	17050

Table 2: *Other parameters from the normalized grayscale MR image (continuation of table 1).*

Metric	Class 1	Class 2	Class 3	Class 4	Class 5
True Positive (TP)	37	43	32	29	48
False Negative (FN)	4	4	5	2	4
False Positive (FP)	3	3	2	6	5
True Negative (TN)	164	158	169	171	151
Sensitivity (TP/(TP+FN))	0.902	0.914	0.864	0.935	0.923
Specificity (TN/(FP+TN))	0.982	0.981	0.988	0.966	0.967
Precision (TP/(TP+FP))	0.925	0.934	0.941	0.828	0.905
Accuracy ((TP+TN)/(P+N))	0.966	0.966	0.966	0.961	0.956
F score (2TP/(2P+FP+FN))	0.913	0.924	0.901	0.878	0.914

Table 3: *Classification rates of an Artificial Neural Network classifier for brain tumour.*

The model uses both neural network and fuzzy logic and it gives good results. With such a low error rate and high accuracy value model proves its superiority even when the available training dataset is not too large.

Conclusion

The classifier obtained 96.34% accuracy on standard dataset for both contrast and non-contrast images. Both contrast and non-contrast images, 96.34% accuracy is obtained on Harvard benchmark dataset. The model helps to classify models by enhancing generalization capability. It helps physicians for treatment based on the type of tumour.

Bibliography

1. Yi-hui Liu., *et al*. "Classification of MR Tumor Images Based on Gabor Wavelet Analysis". *Journal of Medical and Biological Engineering* 32.1 (2011): 22-28.
2. El-Sayed A., *et al*. "A hybrid technique for automatic MRI brain images classification". Studia Univ, Babes Bolyai, Informatica LIV (2009).
3. Evangelia I Zacharaki., *et al*. "MRI-based classification of brain tumor type and grade using SVM-RFE". IEEE International Symposium on Biomedical Imaging (2009): 1035-1038.
4. Whole Brain Atlas: MR brain image (2013).
5. BrainWeb: Simulated Brain MR brain image dataset (2013).
6. The EASI MRI Home: MR brain image (2013).
7. Kamyar Mehran. "Takagi-Sugeno Fuzzy Modeling for Process Control". Industrial Automation, Robotics and Artificial Intelligence, School of Electrical, Electronic and Computer Engineering (2008): 1-21.
8. RL Siegel., *et al*. "Cancer statistics, 2016". *CA: A Cancer Journal for Clinicians* 66.1 (2016): 7-30.
9. RL Siegel., *et al*. "Cancer statistics, 2017". *CA: A Cancer Journal for Clinicians* 67.1 (2017): 7-30.
10. J Liu., *et al*. "A survey of MRI based brain tumor segmentation methods". *Tsinghua Science and Technology* 19.6 (2014): 578-595.
11. Mathur N., *et al*. "Detection of Brain Tumor in MRI Image through Fuzzy-Based Approach". In High-Resolution Neuroimaging-Basic Physical Principles and Clinical Applications; InTech: Rijeka, Croatia (2018).

Volume 4 Issue 3 March 2020